Available online at www.sciencedirect.com
ScienceDirect
Journal of the European Ceramic Society 27 (2007) 4547–4553
www.elsevier.com/locate/jeurceramsoc

Preparation of bioactive sodium titanate ceramics

Inés Becker, Ingo Hofmann *, Frank A. Müller

University of Erlangen-Nuremberg, Department of Materials Science-Biomaterials, Henkestr. 91, 91052 Erlangen, Germany

Received 14 July 2006; received in revised form 4 March 2007; accepted 16 March 2007
Available online 31 May 2007

Abstract

The *in vitro* bioactivity of sol–gel derived sodium titanates with different sodium contents was investigated. Calcined sodium titanates show bioactive behaviour when exposed to simulated body fluid (SBF). A higher sodium content entails higher bioactivity since a higher amount of sodium ions is available for the exchange with H_3O^+ ions from SBF, which results in the formation of Ti–OH groups and subsequently in the formation of an intermediate calcium titanate. The local pH increase triggers the formation of a biomimetic calcium phosphate layer on the surface. Sintering the samples leads to more crystalline sodium tri- and hexatitanate structures and a decrease of the sodium content. The amount of Na^+ ions that can be released from the sodium titanate surface decreases due to a decreasing surface area and the reduced sodium content. As a result bioactivity is lost. Bioactive behaviour can be re-achieved by a subsequent chemical treatment of sintered sodium titanate ceramics in an aqueous NaOH solution.

Keywords: Sol–gel processes; Apatite; $BaTiO_3$ and titanates; Biomedical applications; Bioactivity

1. Introduction

Implant materials, to be used as bone substitutes in load bearing applications, should have the ability to bond to human bone and should have appropriate mechanical properties.[1] The immune system of the human body separates any exogeneous material from the surrounding tissue by developing a connective tissue encapsulation which does not facilitate a firm integration into the surrounding tissue. Therefore, synthetic materials used as bone implants need functional surface groups which allow the formation of a chemical bond between the material and bone. Bioglass, apatite-wollastonite glass–ceramics and sintered hydroxyapatite represent synthetic materials which are able to bond to living bone via the formation of a biologically active hydroxy carbonated apatite (HCA) surface layer.[2–6]

The bioactivity of a material can be tested *in vitro* by using acellular simulated body fluid (SBF) solutions which simulate the inorganic part of human blood plasma.[7] Surface modified titanium, which was submitted to a combined HCl/NaOH treatment, spontaneously forms a HCA layer during soaking in simulated body fluid (SBF).[8,9] It is suggested that the formation of HCA is due to the development of an amorphous sodium titanate gel layer which is formed during the NaOH treatment.[9,10] This gel releases Na^+ ions from its surface into SBF via the exchange with H_3O^+ ions resulting in the formation of Ti–OH groups which act as nucleation sites for HCA.[9,10] Calcium titanate is formed as an intermediate by the reaction of Ti-OH groups with Ca^{2+} ions from SBF.[11] Apatite nucleation is induced by the local pH increase leading to a higher degree of supersaturation with respect to apatite.[9,12]

Bioactive coatings and bulk materials with various compositions were prepared by the sol–gel process.[13–18] Materials prepared by sol–gel processing were shown to be more bioactive compared to those with the same composition but prepared by conventional high temperature fabrication processes.[13,14] The higher amount of hydroxyl groups (Ti–OH and Si–OH) on the surface of materials which were manufactured by sol–gel processing seems to promote the formation of HCA by the subsequent adsorption of Ca^{2+} and PO_4^{3-} ions.[16,17] Sodium titanates were already prepared using different sol–gel precursors.[18–20] The bioactivity of sol–gel prepared sodium titanate gels was investigated by Uchida et al.[18] As prepared sodium titanate gels showed no bioactivity. It was suggested that sodium-containing titania gels that do not contain anatase do not form HCA on their surfaces.[18] Apparently, the Ti–OH groups on titania are effective for apatite nucleation only if arranged in the structural unit of anatase.

* Corresponding author. Tel.: +49 9131 8525545; fax: +49 9131 8525545.
E-mail address: ingo.hofmann@ww.uni-erlangen.de (I. Hofmann).

0955-2219/$ – see front matter © 2007 Elsevier Ltd. All rights reserved.
doi:10.1016/j.jeurceramsoc.2007.03.024

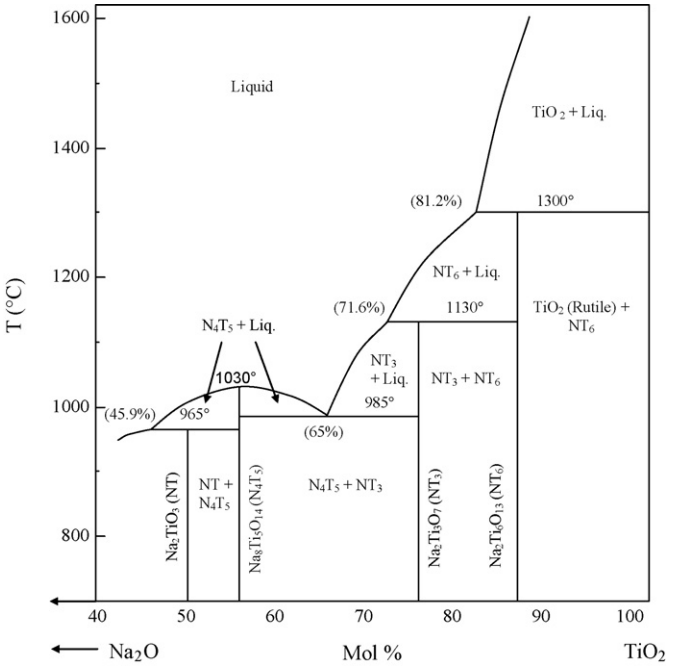

Fig. 1. Phase diagram of the system Na_2O–TiO_2.[21]

In this study, sodium titanate powders of two different compositions, $Na_2Ti_3O_7$ and $Na_2Ti_6O_{13}$, were prepared by using the sol–gel method. The selected compositions are shown in the phase diagram of the system Na_2O–TiO_2 (Fig. 1).[21] The *in vitro* bioactivity of as prepared powders, calcined powders, sintered samples and chemically activated sintered samples was evaluated regarding the HCA forming ability in simulated body fluid (SBF).

2. Materials and methods

2.1. Sample preparation

Powders were prepared by dissolving TiPT (titanium isopropoxide, $Ti(C_3H_7O)_4$, 97%, Alfa Aesar, Germany) in ethanol with a molar ethanol:TiPT ratio of 12.2. Stochiometric amounts of NaOH (≥99%, Carl Roth GmbH & Co. KG, Germany) were dissolved in double distilled water (molar water:TiPT ratio = 197) and subsequently added to the TiPT solution to obtain a fast hydrolysis-condensation reaction. According to the final compositions $Na_2Ti_3O_7$ and $Na_2Ti_6O_{13}$, the molar NaOH:TiPT ratios were set to 0.67 and 0.33, respectively. The prepared suspensions were stirred at 80 °C and then dried by lyophilization for 48 h to prevent agglomeration.

The samples were calcined in air for 4 h with a heating rate of 4 °C/min. Calcination temperatures of 800 °C for $Na_2Ti_3O_7$ and 700 °C for $Na_2Ti_6O_{13}$ were selected according to thermal analyses. Tablets with a diameter of 13 mm and a thickness of 1 mm were uniaxially pressed (115 MPa) using calcined powders and sintered at 1050 °C for 1 h with a heating rate of 4 °C/min. Sintered samples were chemically activated by soaking in 10 M NaOH aqueous solution at 60 °C for 24 h. Subsequently, the samples were rinsed with double distilled water and dried at room temperature.

2.2. In vitro bioactivity tests in SBF

SBF solution was prepared according to a procedure described previously.[22] The solution was buffered at pH 7.3 with tris-hydroxymethyl aminomethane (TRIS) and HCl at 37 °C. NaN_3 was added to inhibit the growth of bacteria. The samples were immersed in SBF under static conditions in a biological thermostat at 37 °C for 7 and 14 days, respectively. The ratio of sample surface area to soaking solution volume S/V was set to 0.04 cm^{-1}. The samples were removed from SBF, washed with double distilled water and dried at room temperature.

2.3. Analysis of samples and SBF

After each step of preparation and treatment the surface of gold sputtered samples was characterized in terms of elemental

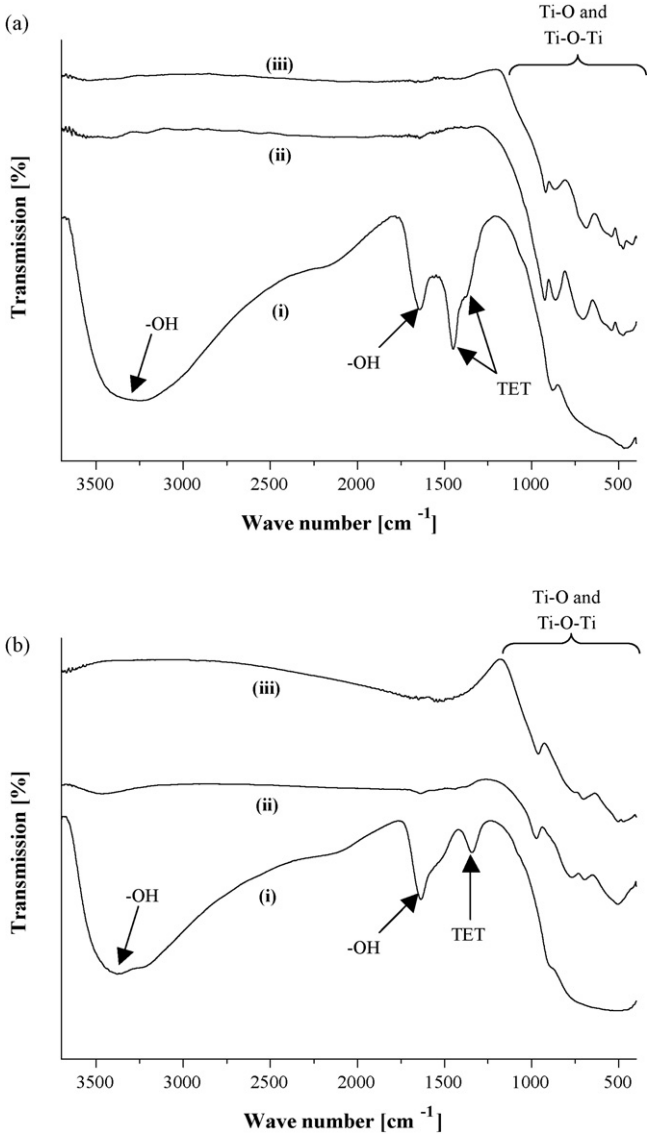

Fig. 2. FTIR spectra of (a) $Na_2Ti_3O_7$ and (b) $Na_2Ti_6O_{13}$ samples: (i) as prepared, (ii) calcined and (iii) sintered for 1 h.

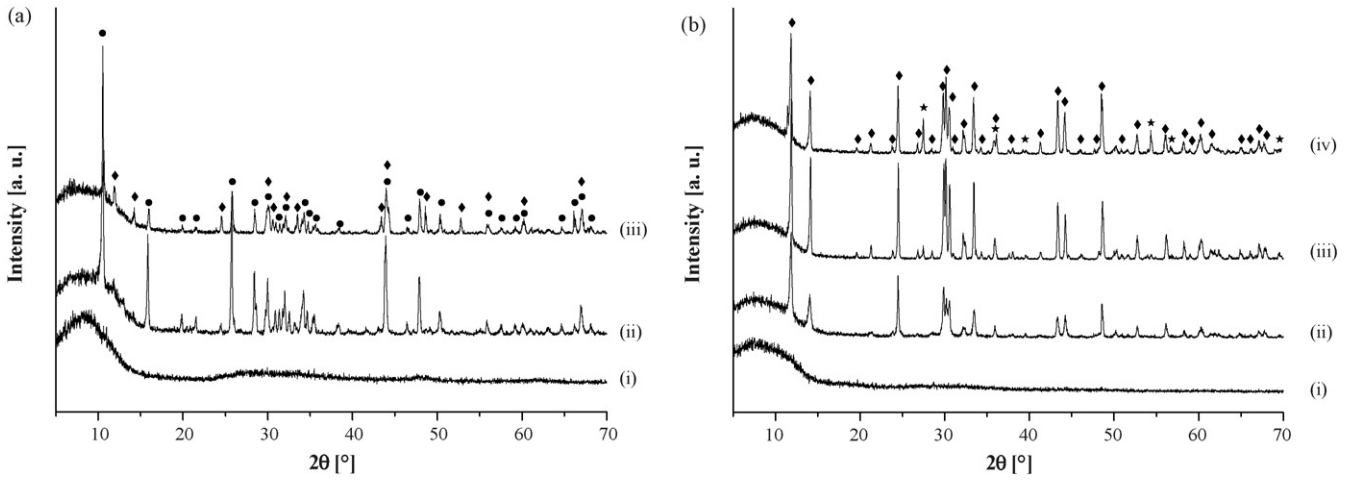

Fig. 3. XRD spectra of (a) $Na_2Ti_3O_7$ and (b) $Na_2Ti_6O_{13}$ samples: (i) as prepared, (ii) calcined, (iii) sintered for 1 h, and (iv) sintered for 2 h; (●) $Na_2Ti_3O_7$, (♦) $Na_2Ti_6O_{13}$ and (⋆) TiO_2 (rutile).

composition and structure using a scanning electron microscope (SEM) (Quanta 200, Fei, CZ) equipped with an energy dispersive X-ray (EDX) analysis unit (INCA x-sight, Oxford Instruments, UK). The apparent density ρ_a of the samples was obtained from measurements of the volume and mass of the pellets. The true density ρ_t of the sodium titanates was determined using helium pycnometry of calcined and grinded powders. The apparent ρ_a and the true density ρ_t were used to calculate the overall porosity P:

$$P = 1 - \frac{\rho_a}{\rho_t} \quad (1)$$

Fourier transform infrared (FTIR) spectra of the samples were acquired using KBr tablets with a sample:KBr mass ratio of 1:300 (Impact 420, Nicolet Instruments, USA). The spectra were measured in the range from 4000 to 400 cm^{-1} with a resolution of 2 cm^{-1}. CO_2 vibration bands were removed from the spectra. Bands were assigned by comparison with literature data.[23–25] X-ray diffraction (XRD) patterns were measured (D-500, Siemens, Germany) using Cu K_α-radiation ($\lambda = 1.5405$ Å) in a 2θ range between 5° and 70°. Step size and measuring speed were set to 0.02° and 1 °/min, respectively. Peak positions given in JPDCS cards ($Na_2Ti_3O_7$: 31-1329, $Na_2Ti_6O_{13}$:

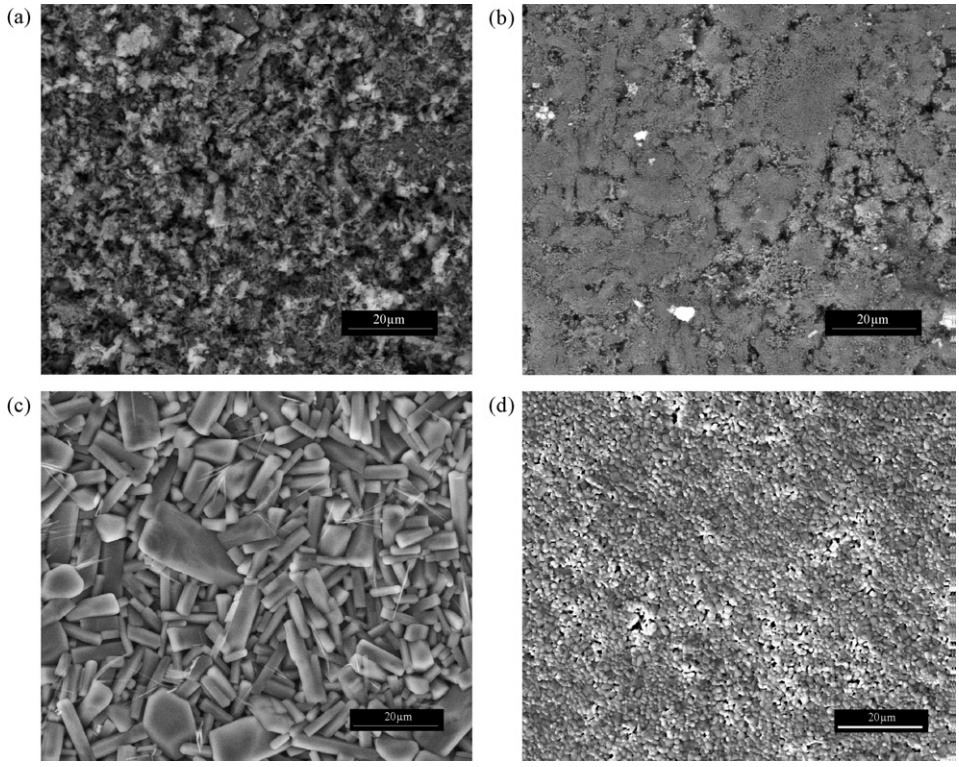

Fig. 4. Scanning electron micrographs of calcined (a and b) and sintered (c and d) samples with different sodium content: (a) and (c) $Na_2Ti_3O_7$ and (b) and (d) $Na_2Ti_6O_{13}$.

73-1398, TiO_2 (anatase): 78-2486, TiO_2 (rutile): 86-0147) were used to identify phases.

Elemental concentrations (Ca and P) and pH of SBF before and after soaking of the substrates were analyzed by inductively coupled plasma-optical emission spectrometry (ICP-OES) (Flame Modula, Spectro Analytical Instruments, Germany) and an electrolyte-type pH meter (720 A+, Thermo Orion, USA).

3. Results and discussion

3.1. Composition of sodium titanates

Fig. 2 shows the FTIR spectra of as prepared, calcined and sintered $Na_2Ti_3O_7$ (Fig. 2a) and $Na_2Ti_6O_{13}$ (Fig. 2b) samples. In the high wave number spectral range, a broad band between 3000 and 3500 cm^{-1} was assigned to fundamental stretching vibrations of different O–H hydroxyl groups (free or bounded) for as prepared samples. Another peak related to O–H hydroxyl groups was found at 1630 cm^{-1} for $Na_2Ti_3O_7$ and 1635 cm^{-1} for $Na_2Ti_6O_{13}$. Bands around 1372 and 1448 cm^{-1} for $Na_2Ti_3O_7$ and 1340 cm^{-1} for $Na_2Ti_6O_{13}$ are related to C–H deformations in tetraethoxytitanate (TET) which forms by the substitution of isopropoxy groups by ethoxy groups when diluting titanium isopropoxide in ethanol.[23] The set of overlapping peaks in the range 800–400 cm^{-1} are related to Ti–O and Ti–O–Ti groups. After calcination and sintering, only Ti–O/Ti–O–Ti vibrations can be observed for both sodium contents.

Fig. 3 shows the XRD patterns of as prepared, calcined and sintered $Na_2Ti_3O_7$ (Fig. 3a) and $Na_2Ti_6O_{13}$ (Fig. 3b) samples. As prepared sodium titanates possess an amorphous structure. Calcination leads to the formation of crystalline $Na_2Ti_3O_7$ and $Na_2Ti_6O_{13}$, respectively. Subsequent heat treatment at 1050 °C leads to the decomposition of $Na_2Ti_3O_7$ to $Na_2Ti_3O_7$ and $Na_2Ti_6O_{13}$. In the case of $Na_2Ti_6O_{13}$ samples, an extension of the sintering time to 2 h leads to the decomposition of $Na_2Ti_6O_{13}$ to $Na_2Ti_6O_{13}$ and rutile (TiO_2). For both types of samples the decomposition seems to be accompanied by the sublimation of Na_2O according to the following equations:

$$2Na_2Ti_3O_7 \rightarrow Na_2Ti_6O_{13} + Na_2O \uparrow \quad (2)$$

$$Na_2Ti_6O_{13} \rightarrow 6TiO_2 + Na_2O \uparrow \quad (3)$$

Thus, the composition of the sample surface is shifted to the TiO_2 rich area of the phase diagram shown in Fig. 1 during sintering.

The average agglomerate size (d_{50}) of calcined powders before calcination amounts to 24.7 μm for $Na_2Ti_3O_7$ and 21.1 μm for $Na_2Ti_6O_{13}$. Fig. 4 shows the microstructure of pellets prepared from calcined powders before (a and b) and after (c and d) sintering. The grain sizes of calcined sodium titanate with the higher sodium content ($Na_2Ti_3O_7$) are in the range of 1 μm, Fig. 4a. The grain sizes of sodium titanate with the lower sodium content ($Na_2Ti_6O_{13}$) are in the submicron range, Fig. 4b. The grain sizes of sintered sodium titanate with the higher sodium content ($Na_2Ti_3O_7$), shown in Fig. 4c, are larger (2–30 μm) compared to those of sodium titanate with the lower sodium content ($Na_2Ti_6O_{13}$) (0.5–3 μm), shown in Fig. 4d. The porosity after sintering is 14.4% for $Na_2Ti_3O_7$ and 21.5% for $Na_2Ti_6O_{13}$.

3.2. Bioactivity of sodium titanates

As prepared samples show no bioactive behaviour after 2 weeks of soaking in SBF, independent of their composition. It can be assumed that after lyophilisation unreacted surface groups like $–C_3H_7$ from TiPT or $–C_2H_5$ from ethanol prevent the deposition of Ca^{2+} ions from SBF to Ti–OH groups and the subsequent formation of apatite. Additionally, the powders have a X-ray amorphous nature. Uchida et al.[18] showed that an amorphous gel does not form apatite in SBF, even though it has abundant Ti–OH groups.

Fig. 5 shows SEM micrographs of surfaces of calcined $Na_2Ti_3O_7$ (Fig. 5a) and $Na_2Ti_6O_{13}$ (Fig. 5b) samples soaked in SBF for 1 week. Both samples are completely covered with

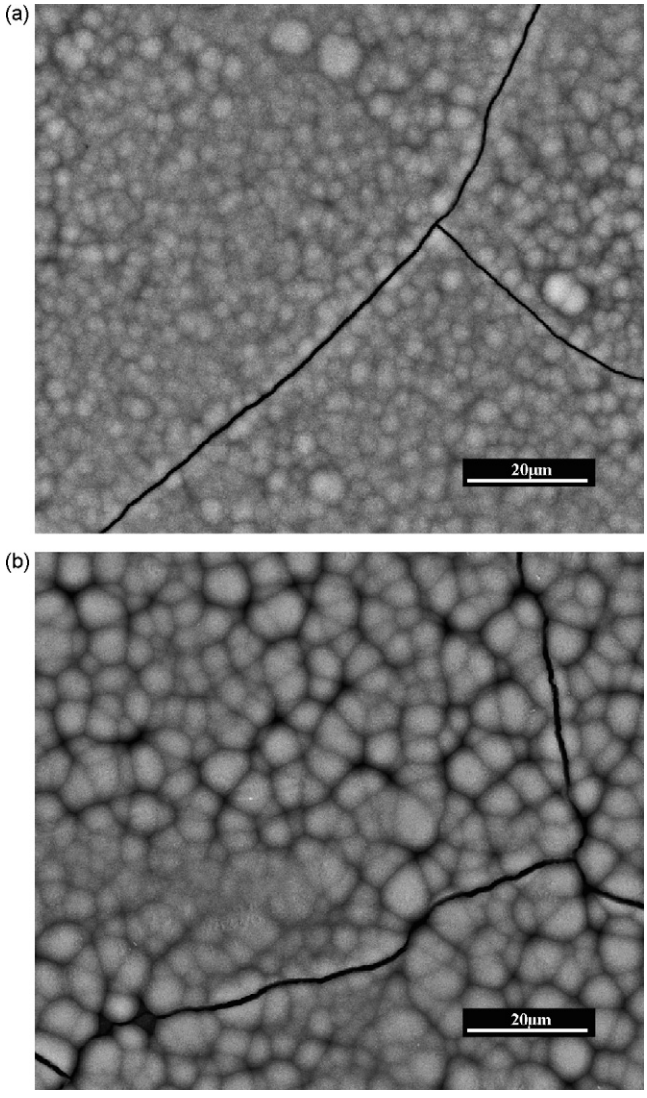

Fig. 5. Scanning electron micrographs of calcined samples with different sodium content after immersion in SBF for 1 week: (a) $Na_2Ti_3O_7$ and (b) $Na_2Ti_6O_{13}$.

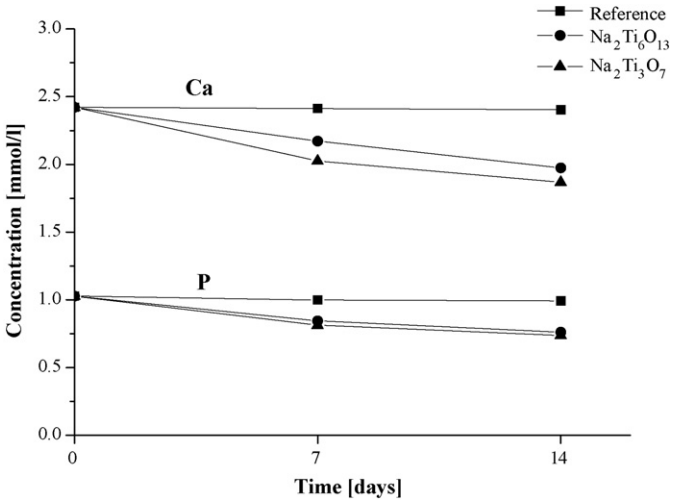

Fig. 6. Changes in Ca and P concentrations during soaking of calcined samples in SBF.

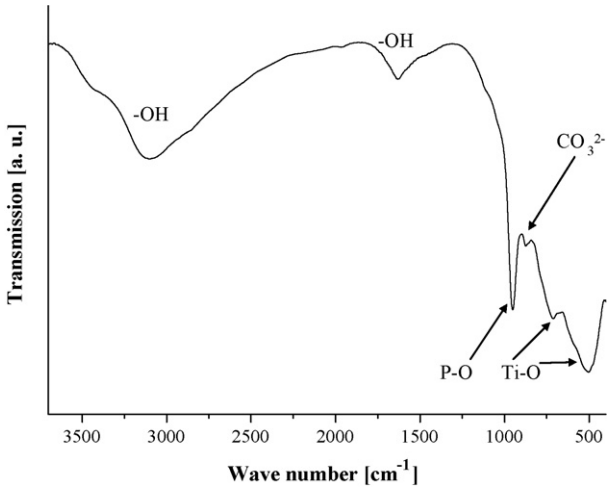

Fig. 7. FTIR spectrum of calcined $Na_2Ti_3O_7$ sample after soaking in SBF for 7 days.

a calcium phosphate layer. Fig. 6 shows the corresponding Ca and P concentrations in SBF after soaking calcined samples. Decreases in Ca and P concentrations are observed indicating that these ions were consumed during apatite crystallization on the substrates. The higher amount of consumed ions for the samples with higher sodium content ($Na_2Ti_3O_7$) indicates their higher degree of bioactivity. Thus, the bioactivity depends on the sodium content in the samples and hence on the ion exchange capacity.

Fig. 7 shows a FTIR spectrum of calcined $Na_2Ti_3O_7$ after soaking in SBF. The broad band between 3000 and 3250 cm^{-1} was assigned to fundamental stretching vibrations of different

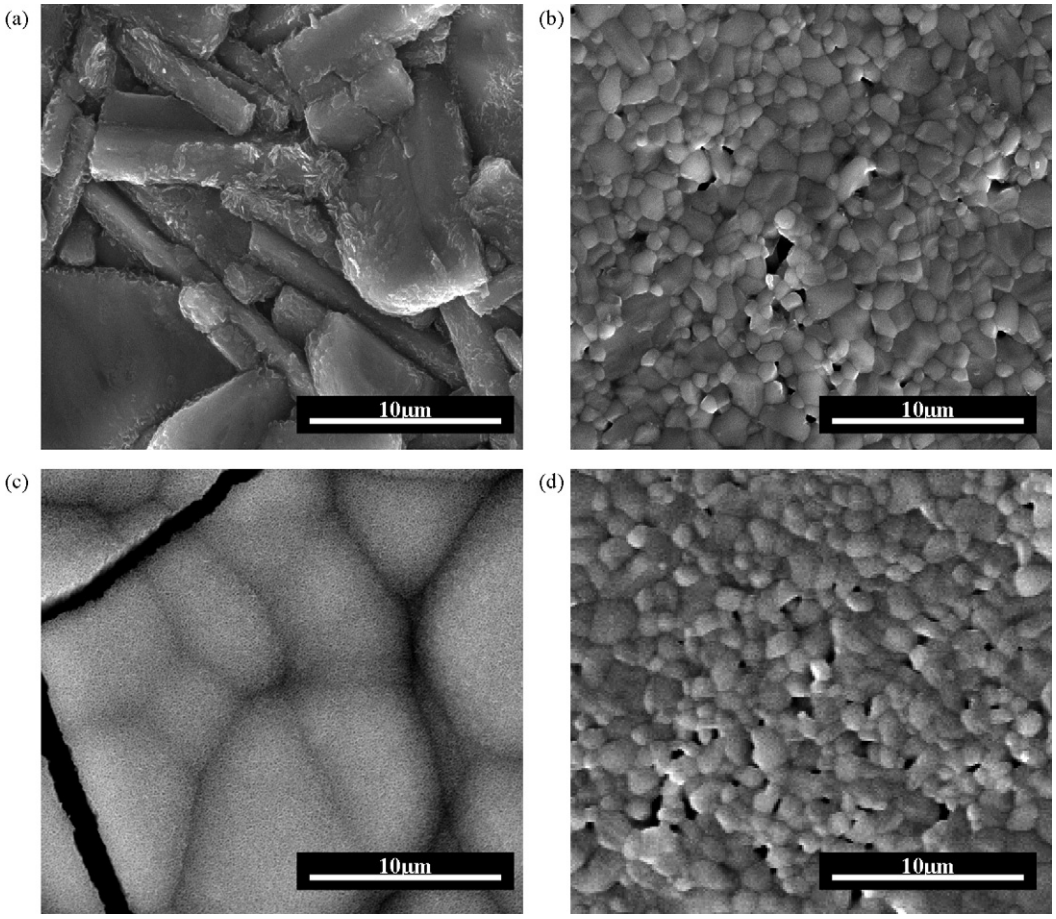

Fig. 8. Scanning electron micrographs of sintered samples (a) $Na_2Ti_3O_7$ and (b) $Na_2Ti_6O_{13}$, treated in 10 M NaOH, and sintered samples (c) $Na_2Ti_3O_7$ and (d) $Na_2Ti_6O_{13}$, treated in 10 M NaOH and subsequently soaked in SBF for 7 days.

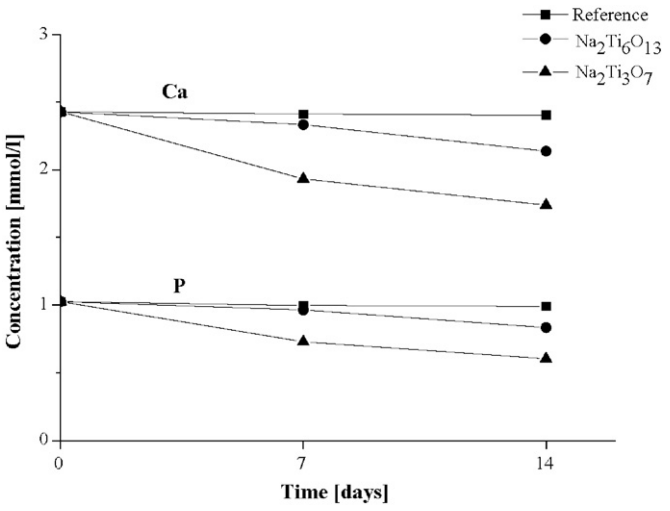

Fig. 9. Changes in Ca and P concentrations during soaking of sintered, NaOH treated samples in SBF.

O–H groups (free or bound). Another peak related to the vibration of hydroxyl groups was found at 1630 cm^{-1}. The peaks at 503 and 712 cm^{-1} are related to Ti–O and Ti–O–Ti vibrations which might overlay the bands of CO_3^{2-} or P–O and O–P–O vibrations. The bands at 874 and 952 cm^{-1} are related to CO_3^{2-} and P–O vibrations, respectively. When exposed to SBF, the sodium titanates release Na^+ ions via exchange with H_3O^+ ions into the solution thereby forming Ti–OH groups on their surface. As a result, pH of the solution and thus the degree of supersaturation with respect to apatite increases. The higher the sodium content in the sample the more Na^+ ions can be exchanged by H_3O^+ ions in the solution and the more Ti–OH groups can be formed which react with Ca^{2+} ions from SBF to form calcium titanate, an intermediate for apatite nucleation.[11]

Sintering of the sodium titanates leads to a decrease of porosity and an increase of density. The sodium content decreases due to decomposition and the release of Na_2O (Eqs. (2) and (3)). Thus, the amount of surface Ti–ONa groups and Ti–OH groups, in contact with SBF, decreases and the available surface area for the ion exchange processes decreases.[26] The rate of Na^+ ion release was reported to decrease with the structural rearrangement from gel to amorphous phase and finally crystalline phase.[27] Sintered sodium titanates were subjected to a NaOH treatment in order to increase the number of Ti–ONa and Ti–OH groups on the surface and, therefore, to re-achieve bioactive behaviour. Fig. 8 shows SEM micrographs of sintered $Na_2Ti_3O_7$ and $Na_2Ti_6O_{13}$ sample surfaces after 10 M NaOH treatment at 60 °C for 24 h (Fig. 8a and b) and after subsequent soaking in SBF (Fig. 8c and d). $Na_2Ti_3O_7$ samples with a high sodium content reveal that the grain boundaries are corroded predominantly as shown in Fig. 8a. Morphological changes were not observed after the NaOH treatment of samples with low sodium content ($Na_2Ti_6O_{13}$) as shown in Fig. 8b. After soaking NaOH treated $Na_2Ti_3O_7$ samples in SBF for 7 days a homogeneous calcium phosphate layer was formed on the surface, Fig. 8c. EDX analysis revealed calcium, phosphorous, sodium, magnesium to be present in the surface. For $Na_2Ti_6O_{13}$, morphological changes were not observed (Fig. 8d) and HCA formation could not be confirmed by EDX analysis. The Ca and P concentrations in SBF after soaking of sintered samples treated in NaOH are shown in Fig. 9. Decreases in Ca and P concentrations are observed indicating that a calcium phosphate was formed on both samples. The decrease of ionic concentrations is significantly more pronounced for $Na_2Ti_3O_7$ samples due to the higher degree of bioactivity.

Sodium titanates consist of negatively charged sheets composed of TiO_6^{8-} octahedra.[28] Depending on the alkali metal content, the titanates adopt different structures, layered or cage structures. Sodium titanates with a high alkali metal content ($Na_2Ti_3O_7$) crystallize in a monoclinic structure that consists of $Ti_3O_7^{2-}$ layers held together with exchangeable sodium cations.[28] At lower sodium contents, hexatitanates ($Na_2Ti_6O_{13}$) with a tunnel structure are formed.[28] Fig. 10 shows schemes of both sodium titanate structures.[19] All Na^+ ions in the layered tri-titanates are accessible for an exchange process with H_3O^+.[28] The stable tunnel structure of the hexa-titanates impedes an ion-exchange of the Na^+ ions.[28]

When the sintered samples are treated with NaOH aqueous solution, some of the Ti–O–Ti bonds could be broken and Ti–O–Na and Ti–OH bonds are formed,[29] according to the fol-

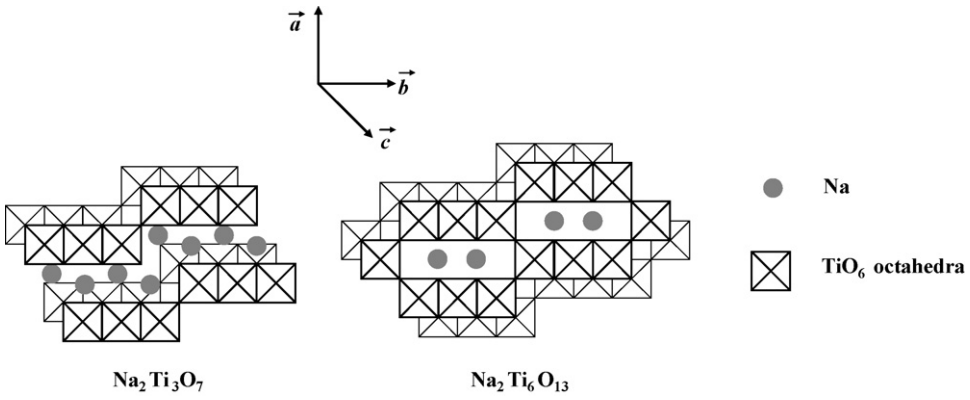

Fig. 10. Schematic drawing of the structures of $Na_2Ti_3O_7$ and $Na_2Ti_6O_{13}$.

lowing equations:

$$\text{Ti–O–Ti} + \text{NaOH} \rightarrow \text{Ti–O–Na} + \text{Ti–O–H} \quad (4)$$

$$\text{Ti–O–Na} + \text{H}_2\text{O} \rightarrow \text{Ti–OH} + \text{NaOH} \quad (5)$$

$$\text{in SBF}: \quad \text{Ti–O–Na} + \text{H}_3\text{O}^+ \rightarrow \text{Ti–OH} + \text{Na}^+ + \text{H}_2\text{O} \quad (6)$$

Soaking the ceramics in NaOH probably increases the amount of Ti–OH groups at the sample surface. According to Eq. (6), Na^+ ions are replaced by H_3O^+ ions in SBF.

The tunnel structure of $Na_2Ti_6O_{13}$ imepedes diffusion and ion exchange processes.[28] Samples with the composition $Na_2Ti_6O_{13}$ therefore are less bioactive than $Na_2Ti_3O_7$ samples with a layer structure.

4. Conclusions

Sodium titanate ceramics were successfully prepared by a sol–gel process and subsequent thermal treatment. Calcined as well as sintered, NaOH treated sodium titanates were shown to form an apatite layer on their surface during *in vitro* bioactivity tests in SBF. The degree of bioactivity increases with increasing sodium content. The structure of $Na_2Ti_3O_7$ allows the exchange of Na^+ by H_3O^+ ions in SBF resulting in an increase of the degree of supersaturation with respect to apatite. The treatment of sintered $Na_2Ti_3O_7$ in NaOH is a suitable method for providing a ceramic implant with bone-bonding ability.

References

1. Kokubo, T., Miyaji, F., Kim, H. M. and Nakamura, T., Spontaneous formation of bonelike apatite layer on chemically treated titanium metals. *J. Am. Ceram. Soc.*, 1996, **79**, 1127–1129.
2. Ogino, M., Ohuchi, F. and Hench, L. L., Compositional dependence of the formation of calcium phosphate films on Bioglass. *J. Biomed. Mater. Res.*, 1980, **14**(1), 55–64.
3. Clupper, D. C., Hench, L. L. and Melchowsky, J. J., Strength and toughness of tape cast bioactive glass 45S5 following heat treatment. *J. Eur. Ceram. Soc.*, 2004, **24**(10–11), 2929–2934.
4. Kitsugi, T., Yamamuro, T., Nakamura, T. and Kokubo, T., Bone bonding behavior of MgO–CaO–SiO_2–P_2O_5–CaF_2 glass (mother glass of AW-glass–ceramics). *J. Biomed. Mater. Res.*, 1989, **23**(6), 621–648.
5. Neo, M., Nakamura, T., Ohtsuki, C., Kokubo, T. and Yamamuro, T., Apatite formation on three kinds of bioactive material at an early stage in vivo: a comparative study by transmission electron microscopy. *J. Biomed. Mater. Res.*, 1993, **27**(8), 999–1006.
6. Landi, E., Tampieri, A., Celotti, G. and Sprio, S., Densification behavior and mechanisms of synthetic hydroxyapatites. *J. Eur. Ceram. Soc.*, 2000, **20**(14–15), 2377–2387.
7. Kokubo, T., Surface chemistry of bioactive glass–ceramics. *J. Non-Cryst. Solids*, 1990, **120**, 138–151.
8. Jonášová, L., Müller, F., Helebrant, A., Strnad, J. and Greil, P., Hydroxyapatite formation on alkali-treated titanium with different content of Na^+ in the surface layer. *Biomaterials*, 2002, **23**, 3095–3101.
9. Jonášová, L., Müller, F., Helebrant, A., Strnad, J. and Greil, P., Biomimetic apatite formation on chemically treated titanium. *Biomaterials*, 2004, **25**, 1187–1194.
10. Liang, F., Zhou, L. and Wang, K., Apatite formation on porous titanium by alkali and heat-treatment. *Surf. Coat. Technol.*, 2003, **165**, 133–139.
11. Takadama, H., Kim, H.-M., Kokubo, T. and Nakamura, T., An X-ray photoelectron spectroscopy study of the process of apatite formation on bioactive titanium metal. *J. Biomed. Mater. Res.*, 2001, **55**(2), 185–193.
12. Kim, H. M., Miyaji, F., Kokubo, T., Nishiguchi, S. and Nakamura, T., Graded surface structure of bioactive titanium prepared by chemical treatment. *J. Biomed. Mater. Res.*, 1999, **45**, 100–107.
13. Haddow, D. B., James, P. F. and van Noot, R., Characterization of sol–gel surfaces for biomedical applications. *J. Mater. Sci. Mater. Med.*, 1996, **7**, 255–260.
14. Peltola, T., Patsi, M., Rahiala, H., Kangasniemi, I. and Yli-Urpo, A., Calcium phosphate induction by sol–gel derived titania coatings on titanium substrate in vivo. *J. Biomed. Mater. Res.*, 1998, **3**, 504–510.
15. Martin, A. I., Salinas, A. J. and Vallet-Regi, M., Bioactive and degradable organic–inorganic hybrids. *J. Eur. Ceram. Soc.*, 2005, **25**(16), 3533–3538.
16. Hench, L. L., Sol–gel materials for bioceramic applications. *Curr. Opin. Solid State M.*, 1997, **2**, 604–610.
17. Li, P. and de Groot, K., Calcium phosphate formation within sol–gel prepared titania in vitro and in vivo. *J. Biomed. Mater. Res.*, 1993, **27**, 1495–1500.
18. Uchida, M., Kim, H. and Kokubo, T., Apatite-forming ability of sodium-containing titania gels in a simulated body fluid. *J. Am. Ceram. Soc.*, 2001, **84**, 2969–2974.
19. Ramírez-Salgado, J., Djurado, E. and Fabry, P., Synthesis of sodium titanate composites by sol–gel method for use in gas potentiometric sensors. *J. Eur. Ceram. Soc.*, 2004, **24**(8), 2477–2483.
20. Yada, M., Goto, Y., Uota, M., Torikai, T. and Watari, T., Layered sodium titanate nanofiber and microsphere synthesized from peroxotitanic acid solution. *J. Eur. Ceram. Soc.*, 2006, **26**(4–5), 673–678.
21. Bouaziz, R. and Mayer, M., The binary sodium oxide-titanium dioxide. *C. R. Hebd. Seances Acad. Sci. C*, 1971, **272**, 1874–1877.
22. Müller, L. and Müller, F., Preparation of SBF with different HCO_3^- content and its influence on the composition of biomimetic apatites. *Acta Biomater.*, 2006, **2**, 181–186.
23. Burgos, M. and Langlet, M., The sol–gel transformation of TIPT coatings: a FTIR study. *Thin Solid Films*, 1999, **349**, 19–23.
24. Djaoued, Y., Taj, R., Brüning, R., Badilescu, S., Ashrit, P. V., Bader, G. and Vo-Van, T., Study of the phase transition and the thermal nitridation of nanocrystalline sol–gel titania films. *J. Non. Cryst. Solids*, 2002, **297**, 55–66.
25. Koutsopoulos, S., Synthesis and characterization of hydroxyapatite crystals: a review study on the analytical methods. *J. Biomed. Mater. Res.*, 2002, **62**(4), 600–612.
26. Yang, J., Li, D., Wang, X., Yang, X. and Lu, L., Study on the synthesis and ion-exchange properties of layered titanate $Na_2Ti_3O_7$ powders with different sizes. *J. Mater. Sci.*, 2003, **38**, 2907–2911.
27. Kim, H. M., Miyaji, F. and Kokubo, T., Effect of heat treatment on apatite-forming ability of Ti metal induced by alkali treatment. *J. Mater. Sci. Mater. Med.*, 1997, **8**, 341–347.
28. Papp, S., Kõrösi, L., Meynen, V., Cool, P., Vansant, E. F. and Dékány, I., The influence of temperature on the structural behaviour of sodium tri- and hexa-titanates and their protonated forms. *J. Solid State Chem.*, 2005, **178**, 1614–1619.
29. Kasuga, T., Hiramatsu, M., Hoson, A., Sekino, T. and Niihara, K., Titania nanotubes prepared by chemical processing. *Adv. Mater.*, 1999, **11**, 1307–1311.